coatings

MDPI

Article

Synthesis, Characterization, and Corrosion Inhibition Potential of Novel Thiosemicarbazone on Mild Steel in Sulfuric Acid Environment

Qusay A. Jawad [1,2], Dhafer S. Zinad [3], Rawaa Dawood Salim [4], Ahmed A Al-Amiery [1], Tayser Sumer Gaaz [5,*], Mohd S. Takriff [6] and Abdul Amir H. Kadhum [6]

1 Energy and Renewable Energies Technology Center, University of Technology, Baghdad 10001, Iraq; 11018@uotechnology.edu.iq (Q.A.J.); dr.ahmed1975@gmail.com (A.A.A.-A.)
2 Electrical Engineering Department, University of Technology, Baghdad 10001, Iraq
3 Applied Science Department, University of Technology, Baghdad 10001, Iraq; dhafer.utech.78@gmail.com
4 Electrical Engineering Technical College, Middle Technical University, Baghdad 10001, Iraq; rawaadawood@mtu.edu.iq
5 Department of Machinery Equipment Engineering Techniques, Technical College Al-Musaib, Al-Furat Al Awsat Technical University, Al-Musaib, Babil 51009, Iraq
6 Department of Chemical & Process Engineering, Faculty of Engineering & Built Environment, Universiti Kebangsaan Malaysia, Bangi, Selangor 43600, Malaysia; sobritakriff@ukm.edu.my (M.S.T.); amir8@ukm.edu.my (A.A.H.K.)
* Correspondence: taysersumer@atu.edu.iq or taysersumer@gmail.com; Tel.: +96-4773-764-8546

Received: 15 July 2019; Accepted: 16 September 2019; Published: 4 November 2019

Abstract: Corrosion of a material by reaction with a corrosive environment is a common problem across many industries. Iraq is an oil country and corrosion represents a large portion of the total costs for oil producing and a natural potential hazard associated with oil production and transportation. The synthesis of novel thiosemicarbazone, namely 2-(2,4-dimethoxybenzylidene)hydrazinecarbothioamide (DMBHC), was conducted and the chemical structure was elucidated via the ^{1}H and ^{13}C NMR (Nuclear magnetic resonance), and FT-IR (Fourier-transform infrared) spectroscopic spectroscopic techniques in addition to carbon, hydrogen, and nitrogen analyses (CHN analyses). The inhibition properties of the investigated thiosemicarbazone were evaluated for mild steel (MS) corrosion in 1N H_2SO_4 using electrochemical impedance spectroscopy (EIS), weight loss method, and scanning electron microscopy (SEM). Electrochemical and weight loss techniques revealed that the tested thiosemicarbazone acted as a superior inhibitor for the acidic corrosion of MS and the efficiency increased with increasing concentrations. The EIS results revealed that thiosemicarbazone demonstrated the highest inhibition efficiency of 94.86%, at a concentration of 0.5 mM. Results from the weight loss technique suggested that the thiosemicarbazone acted as a mixed type corrosion inhibitor. The impact of temperature on the mechanism of inhibition of the new synthesized inhibitor of the surface of MS in 1N H_2SO_4 was investigated at various temperatures (30–60 °C) where the inhibitive efficiency diminished with increasing temperatures. The mechanism of inhibition was additionally verified with the methodological data.

Keywords: impedance; SEM; temperature; inhibitor; isotherm

1. Introduction

Mild steel contains a large proportion of the element iron, which has a wide application in industries, constructional materials, and machines due to its low cost and superior mechanical properties despite its tendency to corrode in aquatic environments, especially in acid solutions [1–3].

Corrosions of mild steel and other alloy surfaces in corrosive environments (sulfuric acid) are typical uniform corrosion examples [4]. The acidic environment, especially sulfuric and hydrochloric acids, is widely used in industrial fields such as pickling and cleaning operations as well as the use of citrus in boilers for de-sedimentation as well as the acidification of oil drilling in oil wells. One of the most important ways of protecting metals in an acidic environment from corrosion is to use organic inhibitors, where the authors in [5] also investigated the reduction of the consumption of acid that occurs during corrosion. H_2SO_4 is the most commonly utilized chemical in the world and is utilized in almost all industries such as steel manufacturing, iron and steel pickling, gasoline, regeneration of ion exchange resins, pharmaceuticals, sugar bleaching, sulfonation agents, fertilizers, automobile batteries, paper bleaching, cellulose fibers, water treatment, amino acid intermediates, and coloring agents [6]. In general, H_2SO_4 is utilized as a pickling solution for steel alloys [7]. Sulfuric acid (H_2SO_4) is also a significant mineral acid that has considerable uses in the same fields and has led researchers to investigate the effect of corrosion inhibitors. Tan [8] studied the inhibition impact of organic compounds on metals in H_2SO_4. It is broadly acknowledged that natural inhibitors show corrosion through adsorption. The inhibitive mechanism is a separation procedure that includes: (i) the inhibitor molecules are adsorbed on the alloy surface forming a tight protective thin layer and (ii) inhibitor molecules are formed on the surface of the alloys, and are efficient in an acidic environment to form a protective layer or remove acid compounds [9–11]. Adsorption, on the other hand, can be described through two major sorts of interaction: chemisorption and physisorption [12–15]. Organic inhibitors act via forming a layer on the mild steel surface and act as an anodic and/or cathodic corrosion inhibitor. This protective layer occurs with the presence of strong interactions, like pi-electrons adsorption, chemisorption, and electrostatic adsorption, which block the acid from attacking the surface of mild steel [16].

The inhibition efficiencies of organic molecules depend on the adsorption abilities in addition to structural, mechanical, and chemical properties of the adsorption layer produced under a particular solution [17]. Generally, an effective organic corrosion inhibitor has sulfur, oxygen, and/or nitrogen atoms in the molecular structure and a hydrophobic moiety that will block the mild steel surface against the corrosive environment. However, the polar moieties in the organic inhibitor molecules are considered to be responsible for forming the adsorption film [18].

In general, the inhibition performance [19] increases in the order oxygen < nitrogen < sulfur due to their increasing propensity to make coordination bonds. Inhibitor molecules with many heteroatoms demonstrate the best corrosion inhibition in comparison to those that only have one of heteroatom. Among such corrosion inhibitors, thiosemicarbazides, especially Schiff bases, are reported as active inhibitors for various alloy−environment systems such as MS, [20–22] aluminum, [23,24] copper, [25,26], and zinc [27] in various corrosive environments. Schiff bases have a privileged position in the field of corrosion inhibition because they are environmentally friendly and can be easily manufactured from low cost raw materials [28–30]. Schiff bases are extremely dense and continuous films on the metal surface, thus reducing the corrosion rate and increasing the inhibition efficacy by delaying anodic and/or cathodic reactions.

Chemisorption involves a charge exchange from inhibitor molecules to the mild steel surface in order to form coordination bonds. This type of adsorption is recognized to have a lot more grounded adsorption energy when compared with the other technique of adsorption. Accordingly, such bonds progress gradually at higher temperatures. Physisorption involves the electrostatic interactions between electric charges on the adsorbed inhibitor molecules and the electric charge at the mild steel surface/solution interface. This process is determined from the values of standard free energy (ΔG°) values that are over −20 kJ /mol with the application of different adsorption models with coefficients of determination close to 1. It should be noted that the previous studies mostly included the use of previously prepared compounds or the use of plant extracts, while the novelty of this report lies in the synthesis of a new anti-corrosion, inexpensive inhibitor, synthesized from a known chemical compound in addition to the involvement of different criteria. The inhibition efficiency was monitored with respect

to concentration, time, and temperature. The aim of this research was to identify and characterize cheap and environmentally friendly solutions to control corrosion that must also be sustainable. Compounds with sulfur atoms are preferred for H_2SO_4, whereas that with a nitrogen-containing function are more efficient in HCl [31]. In the continuation of previous studies [32–36], we report on the synthesis and characterization of a new inhibitor derived from thiosemicarbazide. The novelty of this work lies in the synthesis, characterization (spectral techniques and CHN analysis), and employment of novel thiosemicarbazone as a corrosion inhibitor for the protection of mild steel in a 1N H_2SO_4 solution. The benefit of this thiosemicarbazone is its high inhibition efficiency (94%), low inhibitor concentration, long working period, and strong bonds between the mild steel surface and inhibitor molecules.

2. Experimental

The utilized compounds in this investigation were reagent grade (provided through Sigma-Aldrich, KL, Malaysia) and utilized as provided without further purification. The FTIR (Fourier-transform infrared) spectra were recorded utilizing a Thermo Scientific Model Nicolate 6700 spectrophotometer (Thermo Nicolet Corp., Madison, WI, USA). NMR (Nuclear magnetic resonance) spectra were measured on an AVANCE III 600 MHz spectrometer (Bruker, Billerica, MA, USA). CHN (carbon hydrogen and nitrogen) elemental microanalysis was performed on an Elementar Vario El III Carlo Erba 1108 elemental analyzer (Carlo Erba Reagenti SpA, Rodano, Italy).

2.1. Chemistry

A solution of thiosemicarbazide (2.0 mM) in methyl alcohol (70 mL) was refluxed with 2,4-dimethoxybenzaldehyde (2.0 mM), for seven hours. After completion of the reaction, the precipitate was filtered, washed with methyl alcohol, and dried to yield 52% of a white solid, melting point: 189–192 °C. The chemical structure of the synthesized inhibitor is demonstrated in Scheme 1. The inhibitor molecule was characterized via spectroscopic techniques namely FTIR, NMR, and CHN (carbon hydrogen and nitrogen) analysis. The CHN and analytical calculation/found for the synthesized inhibitor with the chemical formula $C_{10}H_{13}N_3O_2S$: C, 50.19/49.67; H, 5.48/5.35; N, 17.56/17.44. FTIR: 3411.6, 3289.1 and 3201.7 (N–H), and 1596.4 (C=N). 1H-NMR in DMSO-d6 (ppm): 3.79(s, 3H for OCH_3), 3.81 (s, 3H for OCH_3), 6.63, 6.66, and 7.51 (d,1H for aromatic ring), 8.58 (s,1H for N=CH), and 7.49 (1H for NH). 13C-NMR in DMSO-d6 (ppm): 57.13, 58.03, 103.10, 103.8, 108.87, 130.82, 149.02, 160.22, 163.21, 177.90.

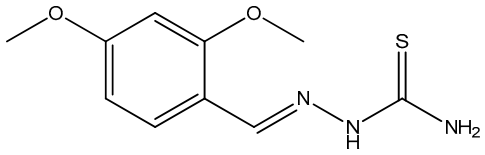

Scheme 1. Chemical structure of the synthesized inhibitor.

2.2. Corrosion Tests

Mild steel samples (Metal Samples Company) with the following chemical composition Fe, 99.21; C, 0.21; Si, 0.38; P, 0.09; S, 0.05; Mn, 0.05; and Al, 0.01 was used for all of the experiments (surface area of 4.5 cm^2). After each immersion time, the mild steel samples were removed and polished mechanically with emery papers, rinsed with double distilled water, degreased with acetone, dried in warm air, and re-weighed according to standard procedure ASTM, G1-03 [37].

2.2.1. Electrochemical Impedance Spectroscopy Measurements

EIS measurements were repeated three times and proceeded in aerated conditions at 30, 40, 50, and 60 °C in 1.0 N sulfuric acid (non-stirred) in the presence of the synthesized inhibitor with the concentrations of 0, 0.1, 0.2, 0.3, 0.4, and 0.5 mM. The H_2SO_4 concentration was chosen based

on the conditions usually performed during the pickling operation in industries. Fresh solutions were prepared utilizing distilled water. Every experiment was repeated three times, and the average value noted the reproducibility of the tests. The investigations were done by employing the Gamry Instrument Potentiostat/Galvanostat/ZRA (REF 600, Gamry Instruments, Warminster, PA, USA) model. The cell contained three electrodes: working (mild steel), counter (a graphite bar), and reference (saturated calomel electrode (SCE)). The DC105 and EIS300 software packages (Gamry) were employed to carry out the electrochemical impedance spectroscopy (EIS) measurements. The measurements started 30 min after the working electrode was immersed in the solution to allow for the stabilization of the steady-state potential.

2.2.2. Weight Loss Measurements

The calculated average values were carried out after repeating each measurement three times. The immersion tests were performed and achieved at temperature levels of 60, 70, 80, and 90 °C with the addition of various concentrations of the inhibitor (0, 0.1, 0.2, 0.3, 0.4, and 0.5 mM). The duration of the immersion times was 1, 5, 10, 24, and 48 h, respectively. Corrosion rates (*CRs*) in (mm/y) and inhibition efficiencies (IE%) in addition to surface coverage (θ) can be calculated according to Equations (1)–(3).

$$C_R(\text{mm/y}) = \frac{KW}{ATD} \quad (1)$$

where K is the constant (87.6); W is the weight loss (mg); A is the area (cm^2); and D is the density (g/cm^3)

$$IE\% = \frac{W_o - W_i}{W_o} \times 100 \quad (2)$$

$$\theta = \frac{W_o - W_i}{W_o} \quad (3)$$

The coupons mass loss is represented as W_o and W_i in the absence and presence of the inhibitor, respectively.

2.3. Scanning Electron Microscope Examination

A SEM, TM1000 Hitachi Tabletop Microscope (Hitachi, Krefeld, Germany) at 2000× magnification, was utilized to investigate the surface of the coupons that were immersed in sulfuric acid in the presence and absence of a corrosion inhibitor for 3 h.

3. Results and Discussion

3.1. Chemistry

The reaction sequences for the synthesis of a new corrosion inhibitor starting from thiosemicarbazide are outlined in Scheme 2. The new synthesized inhibitor (DMBHC) was obtained by refluxing 2,4-dimethoxybenzaldehyde with thiosemicarbazide in methyl alcohol. The FTIR spectrum of DMBHC showed an absorption band at 3411.6 and 3289.1 cm^{-1} for the amino group, 3201.7 cm^{-1} for N-H amine stretching, and 1596.4 cm^{-1} for azomethine C=N. This band confirmed the formation of the Schiff base. The 1H-NMR spectrum exhibited a singlet at δ 3.79 ppm and 3.81 ppm due to the three protons of the methoxy groups, a doublet at 6.63, 6.66, and 7.51 ppm for the aromatic ring protons (d,1H for aromatic ring)., and a singlet at 8.58 ppm for azomethine (s,1H for N=CH), where this band confirmed the formation of the Schiff base. Finally, there was a band at 7.49 ppm for the amino group proton (1H for NH). 13C-NMR in DMSO-d6 (ppm): The spectrum exhibited bands at 57.13 and 58.03 ppm were for carbons of the methoxy groups. The bands at 103.10, 103.8, 108.87, 130.82, 149.02, and 160.22 ppm were for carbons of the aromatic ring. The band at 163.21 ppm was for the carbon of azomethine group, and this band confirmed the formation of the C=N (confirmation) group. Finally, there was a band at 177.90 ppm for the carbon of C=S.

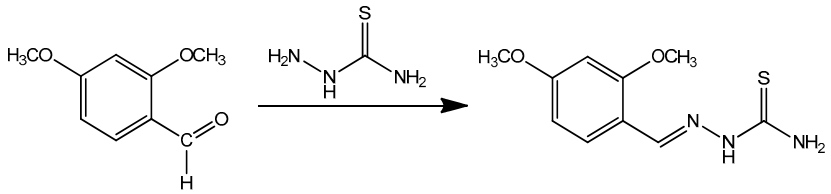

Scheme 2. The synthesis of the corrosion inhibitor.

3.2. Electrochemical Impedance Spectroscopy (EIS)

Mild steel corrosion in a corrosive environment in the presence of the synthesized inhibitor at the concentrations 0.0, 0.10, 0.20, 0.30, 0.40, and 0.50 mM were investigated at temperatures of 30.0, 40.0, 50.0, and 60.0 °C. Electrochemical impedance spectroscopy calculations were conducted by using the AC signals of the 5 mV peak-to-peak amplitude at the frequency range of 100 KHz to 0.1 Hz of corrosion potential. The data of impedance were fit to proper equivalent circuits (ECs) employing the Gamry Echem Analyst software. Figure 1 demonstrates the Nyquist plots for mild steel in a corrosive environment at 30 °C with various concentrations of the synthesized inhibitor (0.0, 0.10, 0.20, 0.30, 0.40, and 0.50 mM). Table 1 shows the CPE matching data for tested coupons in a concentrated sulfuric acid environment.

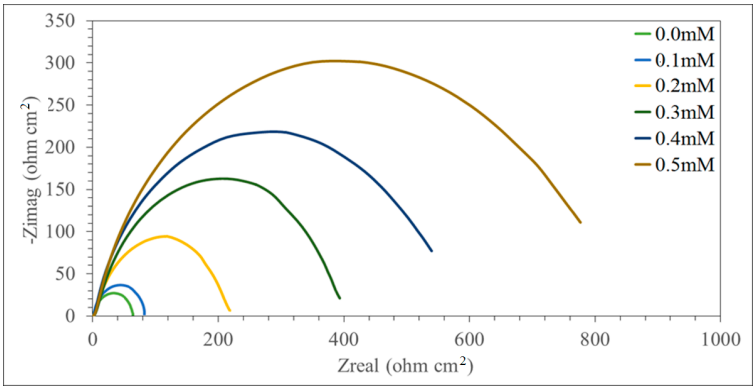

Figure 1. Nyquist plot for MS (Mild steel) in one normal sulfuric acid at various concentrations of DMBHC (2-(2,4-dimethoxybenzylidene)hydrazinecarbothioamide) at 30 °C.

Table 1. CPE (constant phase element) data matching that of MS in a corrosive solution with various concentrations of the DMBHC at 30 °C.

Concentration (mM)	R_s (ohm cm^2)	R_{ct} (ohm cm^2)	C_{dl} (μF cm^{-2})	*IE* (%)
0.0	1.630	46.09	512.2	0.00
0.1	1.716	239.63	375.26	39.43
0.2	1.572	251.52	236.64	72.62
0.3	1.680	433.94	182.03	82.67
0.4	1.655	555.64	153.36	88.49
0.5	1.610	783.61	145.24	94.30

Abbreviations: *IE* is the inhibition efficiency whereas the R_s, R_{ct}, and C_{dl}, are the solution resistance, charge transfer of resistance, and double-layer charge respectively.

According to Figure 1, the increase in impedance can be considerably detected with increasing concentrations of then synthesized inhibitor. Each inhibitor concentration showed a distinctive semicircular graph and the semicircle diameter was related to the inhibitive corrosion rate. The semicircle diameter increased with the increase in the concentration of inhibitor, which means that the rate of corrosion decreased.

From Figure 1, it can be concluded that the impedance response of MS was considerably modified after the addition of DMBHC to the acidic environment. This fact can be attributed to an increase in the

impedance substrate with an increase in the DMBHC concentration. However, the resistance of mild steel in the presence of 0.5 mM of DMBHC decreased with an increasing solution temperature (Figure 2). This conduct is due to the desorption of the adsorbed DMBHC molecules from the surface of the mild steel. In the resistance spectra of the mild steel with DMBHC, the Nyquist schemes included two loops, the first being in the high frequency area (HF) and the second being the intermediate frequency (MF), in conjunction with unreasonable inductive behavior at minor frequencies (LF). HF and MF loops were imposed on the electrode and on the charge transfer method, respectively. Inductive behavior observed in the LF region was attributed to absorption relaxation DMBHC molecules on the surface of the mild steel in the corrosive environment without and with the inhibitor, respectively [18,38]. Comparable conduct was spotted for whole tested temperatures. The working electrode with the corroded surface was predicted to be inhomogeneous due to the roughness, so the capacity was demonstrated by a steady phase element (CPE).

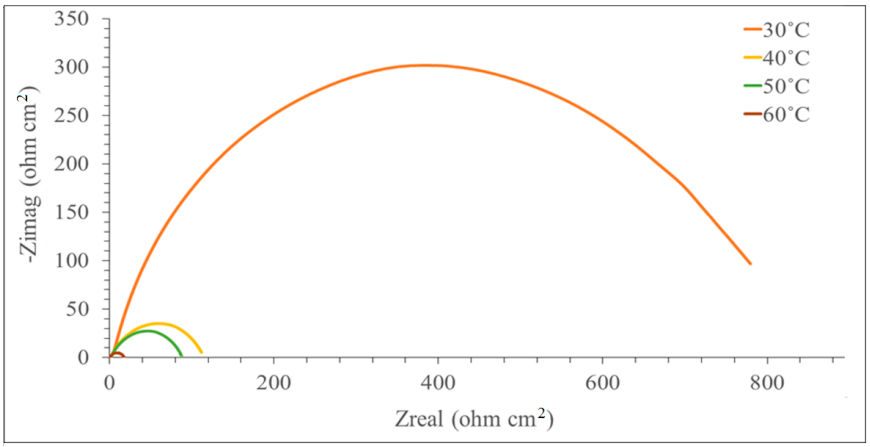

Figure 2. Nyquist plot for mild steel with 0.5 mM of the inhibitor in 1N H_2SO_4 at various temperatures.

A decrease in the C_{dl} value was due to a decrease in the double layer dielectric constant, a decrease in the surface area, or an increase in the double layer thickness. Due to the fact that the process is not under diffusion control, the latter is not possible, and the surface area is, in this case, constant, therefore the decrease in the C_{dl} value was attributed to the replacement of the adsorbed water molecules on the metal surface by the inhibitor having a lower dielectric constant, which indicates that the adsorption of the inhibitor molecules is necessary to decrease the steel corrosion rate.

The corrosion of the MS surface in a corrosive environment with DMBHC was investigated at various temperatures (30.0, 40.0, 50.0, and 60.0 °C). Figure 2 demonstrates the Nyquist plots for MS in the presence of the synthesized inhibitor at the concentration 0.5 mM in 1.0 N sulfuric acid at various temperatures. According to Figure 2, the semicircle diameter became minimal as the temperature was raised from 30.0–60.0 °C. The higher the solution temperature, the smaller the diameter of the semicircle. This consequence implies that the CR (corrosion rate) diminishes with the increasing temperature of the solution [39]. We used Gamry Echem Analyst software to analyze the EIS data of the experiments (CPE, R_s, R_{ct}, and C_{dl}). Table 2 displays the CPE matching data in a corrosive environment in the presence of the inhibitor at the concentration 0.5 mM for mild steel at various temperatures. According to Table 2, a rise in the temperature from 30 °C to 60 °C caused the decreases in R_{ct} and *IE*. The molecules of the corrosion inhibitor adsorbed on the mild steel surface will experience desorption if the temperature of the solution is increased.

Table 2. CPE matching data for MS with 0.5 mM of inhibitor in 1N H_2SO_4 at various temperatures.

Temp. °C	Conc. (mM)	R_s (ohm cm^2)	R_{ct} (ohm cm^2)	C_{dl} (µF cm^{-2})	*IE* (%)
30	0.0	1.630	46.09	512.2	0.00
30	0.5	1.610	783.61	145.24	94.30
40	0.0	1.236	17.64	1229	0.00
40	0.5	1.927	79.34	313.30	85.91
50	0.0	1.114	8.91	1278	0.00
50	0.5	1.372	47.37	341.83	74.93
60	0.0	1063	4.27	1383	0.00
60	0.5	1.689	11.02	658.43	58.32

When the results of the EIS have been obtained, the fitting of the circuit was carried out by utilizing the parabolic circuit model. The CPE circle was selected as an equivalent model for matching performance. In Figure 3, the solution resistance was represented by R_s, where the charge transfer resistance and the constant phase element were represented by R_{ct} and CPE, respectively.

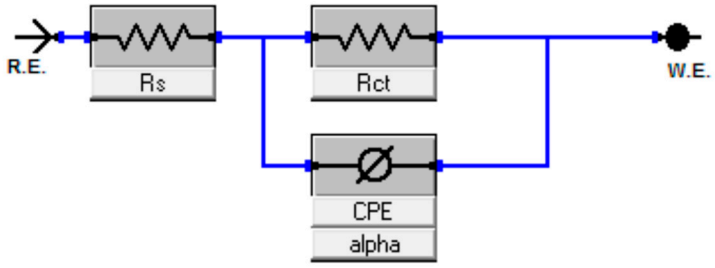

Figure 3. The equivalent circuit model for MS with the inhibitor utilized to fit the impedance data.

EIS data (Nyquist plot, Bode plot) were analyzed and identified as a corrosion mechanism that occurred on the metal surface. EIS data are often interpreted in terms of equivalent electrical circuits that are employed to characterize the electrical features of electrochemical interfaces [40]. Mostly, the impedance spectra obtained for MS corrosion in H_2SO_4 environment consists of one time-constant in Bode-phase representation, which corresponds to the process of a charge/transfer. The MS Bode plots in 1.0 N H_2SO_4 environment in the presence and absence of the DMBHC is demonstrated in Figure 4. When the Nyquist plot had a depressed/semicircle with the center under the real axis, such behavior is characteristic for solid electrodes and is often referred to as frequency dispersion, which can be attributed to the roughness and inhomogeneity of the MS surface [41]. Two routes were utilized in previous studies to characterize the spectra EIS for the inhomogeneous films on the surface of MS or rough and porous electrodes. The first is the limited transmission line model [42], and the second is the filmed equivalent circuit model [43], which is generally suggested for the investigation of the decay of coated alloys [44]. It has been proposed that the EIS spectra for the metal coated by the organic molecules layers are quite comparable to the failed coating alloys.

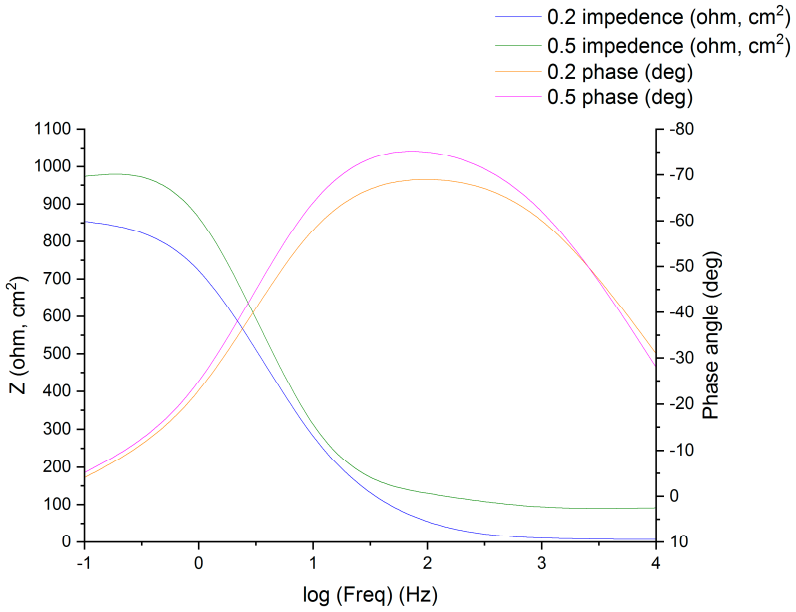

Figure 4. Experimental impedance and phase data in Bode format for mild steel in 1.0 N H_2SO_4 containing the 0.5 mM corrosion inhibitor as denoted by the fitted line using the equivalent circuit.

3.2.1. Open Circuit Potential (OCP)

The OCP was measured at varying temperatures at the fixed inhibitor concentration 0.5 mM. The OCP (Figure 4) increased in the range of 40 and 60 °C, demonstrating that the counterpart sample of mild steel corrosion due to the considerable amounts of protection causing debilitation, and the inhibitor could further expedite the corrosion rate. In other words, a high temperature decreased the effectiveness of the inhibitor [45,46].

From Figure 5, it is obvious that the addition of DMBHC to the sulfuric acid shifted the OCP to more positive values at all investigated temperatures. This positive shift of the OCP in the presence of DMBHC shows that DMBHC influenced the anodic reaction of the MS surface corrosion. At the temperature of 30 °C, the maximum shift was 55 mV. This primary result suggests that DMBHC can block anodic reactions under OCP conditions, leading to the oxidation on the mild steel surface [13]. The OCP values in the presence of DMBHC shifted toward the positive direction with increasing temperatures when considering the deterioration of the surface layers for the DMBHC and oxide.

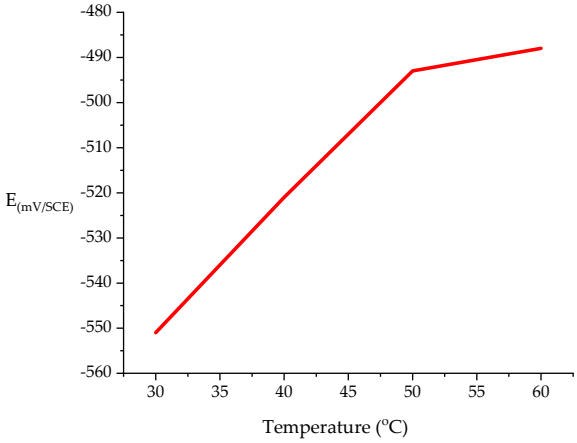

Figure 5. OCP (open circuit potential) as a function of temperature for MS in 1.0 N H_2SO_4 with 0.5 mM corrosion inhibitor.

3.2.2. Weight Loss Studies

Concentration Effect

Differences in CR and IE based on various concentrations of DMBHC inhibitor molecules for immersion times of 1, 5, 10, 24, 48, and 72 h in a sulfuric acid environment at 30 °C are explained in Figures 5 and 6. The corrosion rate decreased with an increase in the DMBHC concentration. The inhibition performance increased with increasing DMBHC concentration. The result showed that the DMBHC molecules were adsorbed on the mild steel surface and formed a protective layer in both low and high concentrations of DMBHC. From Figures 6 and 7, it can be seen that the difference in *CR* and *IE*% with the immersion time became considerable within the first 5 h. At 5 h, as the immersion time was increased, the corrosion rate of DMBHC become the lowest value of 14.25 and the inhibition efficiency reached a superior value of 93.84%. Broadly, the adsorbed of DMBHC molecules are the displacement reaction involving the elimination of adsorbed H_2O molecules from the mild metal surface. DMBHC molecules were adsorbed chemically due to interactions of the pi-electrons of these molecules with the mild steel surface. The *IE* was observed to decrease after 10 h of immersion. The decrease in *IE* was attributed to the desorption of the DMBHC from the MS surface. Generally, the *IE* of DMBHC depends on the ability of adsorption on the surface. The surface coverage (θ) is defined as IE/100 and can be obtained from weight loss technique (Equation (3)).

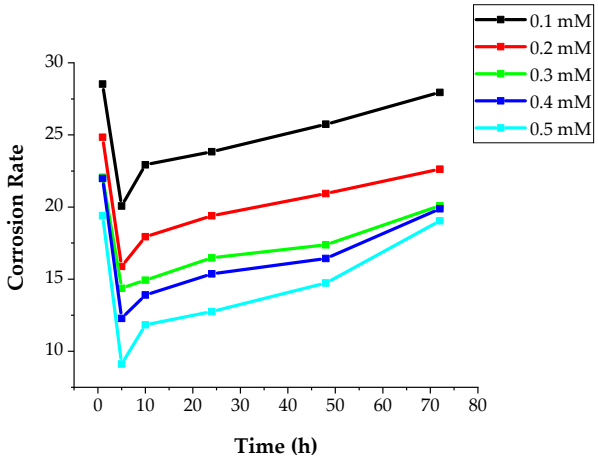

Figure 6. *CR* with various immersion times, h, in 1.0 N H_2SO_4 solution at 30 °C with various concentrations of DMBHC.

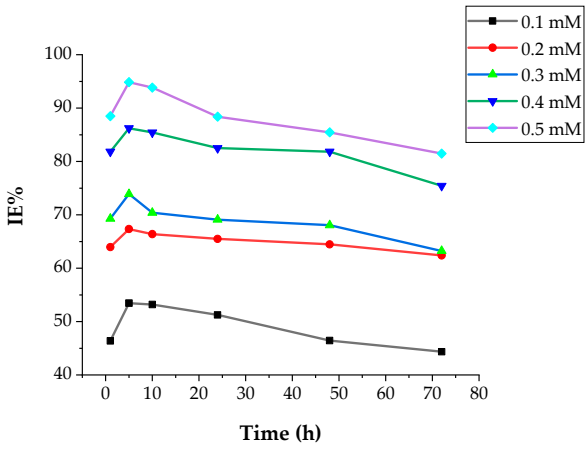

Figure 7. *IE* with various immersion times, h, in 1.0 N H_2SO_4 solution at 30 °C with various concentrations of DMBHC.

Temperature Impact

The influence of temperature was investigated on two factors: corrosion rate and inhibition efficiency. The results are shown in Figure 8. In general, the corrosion rate linearly increased with increasing temperature, as demonstrated in Figure 8. The inhibition efficiency decreased with the increase of temperature. The decrease in the inhibition efficiency of DMBHC at higher temperatures was due to the instability of the DMBHC molecules when these molecules were subjected to higher temperatures. Moreover, the water viscosity was decreased based on the temperature increase, which led to increased diffusion, which would permit the increased transport of reactants and products on the mild steel surface. It is obvious from the results that the impact of temperature on the corrosion rate in the absence of the corrosion inhibitor was 3–4 times that in the presence of the corrosion inhibitor, which was because the inhibitor isolates the metal from the solution. An increase in temperature is normally expected to speed up a chemical reaction according to thermodynamic considerations.

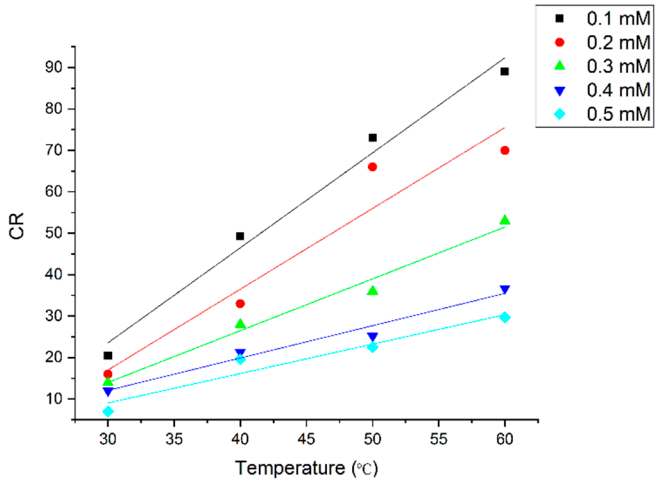

Figure 8. Effect of temperature on *CR* at different concentrations for an immersion time of 5 h.

The effect of temperature on *IE*% is illustrated in Figure 8. It shows a perfect significance for the *IE*% drop with temperature rise due to the physical–chemical adsorption.

Figures 8 and 9 show that a longer immersion time indicates a higher corrosion rate and lower inhibition efficiency, suggesting that the DMBHC molecules may be unstable at longer immersion times. The decrease in inhibition efficiency with time has been attributed to a decrease in the surface coverage with immersion times. These results demonstrate that the adsorption of the DMBHC molecules on the coupon surface is relatively long. That the inhibition efficiencies increase with an increase in concentration demonstrate that the surface coverage by the DMBHC molecules increases.

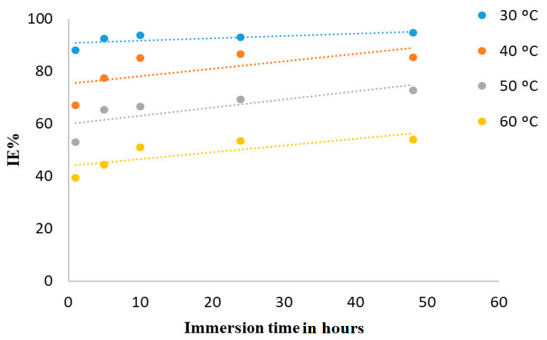

Figure 9. *IE*% vs. different immersion times at various temperatures with a concentration of 0.5 mM in 1N H_2SO_4 solution.

Therefore, surfaces with an incomplete protective layer remain to be exposed to the corrosive environment for a long period of time [47,48].

3.2.3. Inhibitive Mechanism

The corrosion inhibitor could be adsorbed on the mild steel surface and form a protective layer to improve the corrosion impedance of mild steel by decreasing the corrosion rate [37]. In general, the inhibitive mechanism is one of three approaches: (1) the chemical approach (chemisorption), where the inhibitor molecules are adsorbed on the metal surface and form a protective film; (2) the inhibitor molecules lead to the formation of a protective layer through oxide protection of the base metal; and (3) the inhibitor molecules react with the potential corrosive components of the environment and form metal complexes [49]. The initial stage in the mechanism of DMBHC as a corrosion inhibitor in a H_2SO_4 solution is the adsorption of DMBHC molecules on the mild steel surface. In previous studies, the formation of donor–accepter surface complexes between unshared and/or π-electrons of inhibitor molecules and the unoccupied orbital of iron were assumed [50,51]. The adsorption process is affected by the charges and/or nature of the alloy and inhibitor molecular structure with the nature of a corrosive environment. The PZC (potential with zero charge) is the potential of metal which is measured versus the reference electrode that the ionic double layer is absent on the electrode and the electrode has superior capabilities to adsorb material solved in the electrolyte. The power of an electrode to adsorb the inhibitor molecules is redacted with the existence of the potential variation on the ionic double layer. This is due to the field pulls in H_2O molecules with a superior electric constant, dislodging complexes from the mild steel surface. Consequently, the adsorption power of an electrode is extremely close to the zero charge. The charge of the surface can be determined [35] from the PZC on the ψ_c (correlative scale) through Equation (4):

$$\psi_c = E\text{corr} - Eq = 0 \quad (4)$$

where $Eq = 0$ is the PZC. However, the value of Ecorr obtained in acid is −441 mV versus SCE [52–55].

The sulfuric acid ψ_c value is positive, so the surface of mild steel achieves a positive charge. Sulfate ions (in the H_2SO_4 environment) are initially adsorbed on the mild steel surface, therefore, the surface becomes negatively charged. Due to the electrostatic attraction, the synthesized inhibitor molecules are adsorbed on the mild steel surface with predictable high inhibition efficiency. The DMBHC is adsorbed on the MS surface through pi and free electrons and exhibits a higher performance in sulfuric acid.

Electrostatic interaction, chemisorption of the DMBHC molecules, is possible via the unoccupied (d) orbital of Fe-atoms, which acts as an electron acceptor. Therefore, coordinated bonds are formed through the overlap of the unoccupied 3d-orbitals of iron with p-orbital electrons in the DMBHC molecules. Thus, DMBHC molecules can be adsorbed on a metal surface.

DMBHC molecules against MS corrosion in 1N of H_2SO_4 can be expounded in terms of the number of adsorption sites, charge density, size of the molecules, interaction of the inhibitor with the surface of the metal technique, and formation of an insoluble complex. From chemical bonds with a metallic surface, the π-electrons involved in both unpaired electrons and double bonds on nitrogen and oxygen atoms are displayed in Scheme 3.

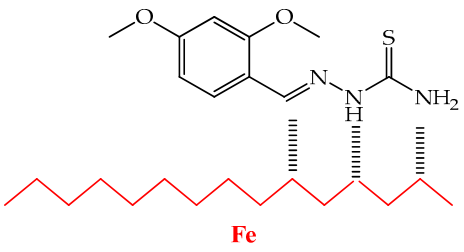

Scheme 3. The proposed action of the DMBHC molecule mechanism as a corrosion inhibitor.

3.2.4. Scanning Electron Microscopy (SEM)

The scanning electron microscope was located in the Unit of Electron Microscopy at the Universiti Kebangsaan Malaysia. Figure 10 shows the micrograph of the coupon surface where it can be observed that the surface was corroded and rough in the corrosive solution in the absence of the corrosion inhibitor. The metal surface was extremely attacked by sulfuric acid. In Figure 11, the metal surface was not considerably affected by corrosion due to formation of a protection film on the metal surface. This suggests that the synthesized corrosion inhibitor has the ability to inhibit the pitting corrosion of a metal surface in a 1N H_2SO_4 environment.

Figure 10. The SEM micrograph for mild steel in a corrosive solution in the absence of the corrosion inhibitor.

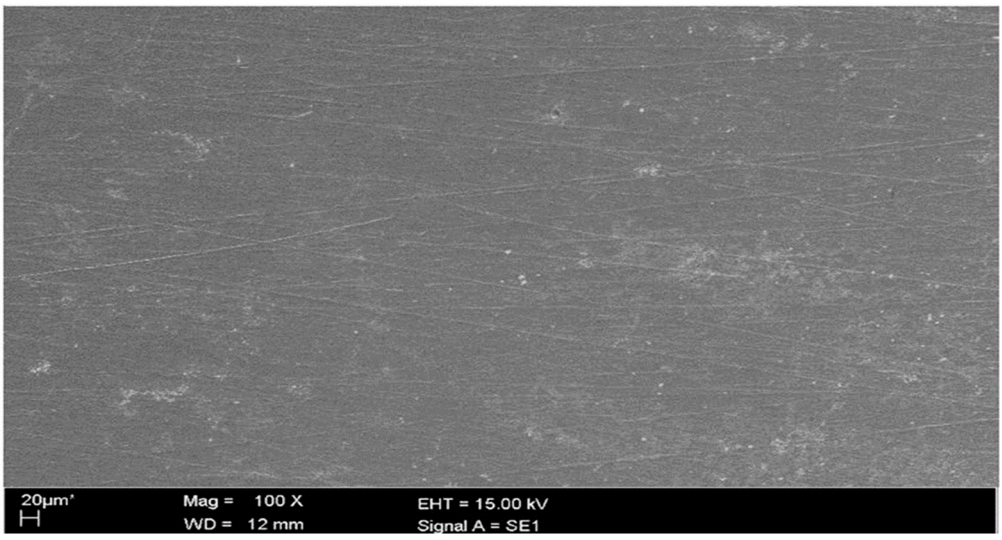

Figure 11. The SEM micrograph for mild steel in a corrosive solution in the presence of the corrosion inhibitor.

4. Conclusions

In this investigation, a new corrosion inhibitor was synthesized and the structural formula was elucidated via deferent spectroscopic measurements. Variation in the EIS and the weight loss method were employed to investigate the corrosion inhibition of MS in a corrosive environment at 30, 40, 50 and 60 °C. The new inhibitor demonstrated superior inhibition effectiveness as a mixed-type inhibitor.

Generally, the corrosive corrosion of MS was increased proportionally with temperature. The SEM micrographs explained that the molecules of the inhibitor formed a layer to protect the surface of the mild steel surface against the corrosive solution and demonstrated the highest inhibition performance of 93%.

Author Contributions: Conceptualization, Q.A.J. and D.S.Z.; Methodology, Q.A.J. and D.S.Z.; Software, T.S.G.; Validation, R.D.S., Q.A.J. and T.S.G.; Formal Analysis, A.A.H.K.; Investigation, M.S.T.; Resources, A.A.H.K.; Data Curation, R.D.S.; Writing—Original Draft Preparation, A.A.A.-A.; Writing—Review & Editing, A.A.A.-A. and T.S.G.; Supervision, A.A.H.K.; Funding Acquisition, M.S.T.

Funding: This research was funded by Universiti Kebangsaan Malaysia, Grant No. 020-2017.

Acknowledgments: The authors thank the UKM-YSD Chair on Sustainable Development for the Grant 020-2017 "Malaysia" for supporting this work.

Conflicts of Interest: The authors declare no conflicts of interest.

References

1. Ahmed, M.H.O.; Al-Amiery, A.; Al-Majedy, Y.K.; Kadhum, A.A.H.; Mohamad, A.B.; Gaaz, T.S. Synthesis and characterization of a novel organic corrosion inhibitor for mild steel in 1 M hydrochloric acid. *Results Phys.* **2018**, *8*, 728–733. [CrossRef]
2. Al-Amiery, A.; Kassim, F.A.B.; Kadhum, A.A.H.; Mohamad, A.B. Synthesis and characterization of a novel eco-friendly corrosion inhibition for mild steel in 1 M hydrochloric acid. *Sci. Rep.* **2016**, *6*, 19890. [CrossRef] [PubMed]
3. Al-Amiery, A.; Kadhum, A.; Mohamad, A.; Junaedi, S. A novel hydrazinecarbothioamide as a potential corrosion inhibitor for mild steel in HCl. *Materials* **2013**, *6*, 1420–1431. [CrossRef] [PubMed]
4. Rubaye, A.; Abdulwahid, A.; Al-Baghdadi, S.B.; Al-Amiery, A.; Kadhum, A.; Mohamad, A. Cheery sticks plant extract as a green corrosion inhibitor complemented with LC-EIS/MS spectroscopy. *Int. J. Electrochem. Sci.* **2015**, *10*, 8200–8209.
5. Trabanelli, G. Inhibitors An Old Remedy for a New Challenge. *Corrosion* **1991**, *47*, 410–419. [CrossRef]
6. Data Research Analyst. Worldofchemicals.com. Available online: https://www.worldofchemicals.com/430/chemistry-articles/industrial-applications-of-sulfuric-acid.html (accessed on 15 August 2019).
7. Bentiss, F.; Lagrenee, M.; Traisnel, M.; Hornez, J.C. The corrosion inhibition of mild steel in acidic media by a new triazole derivative. *Corros. Sci.* **1999**, *41*, 789. [CrossRef]
8. Tan, B.; Zhang, S.; Qiang, Y.; Feng, L.; Liao, C.; Xu, Y.; Chen, S. Investigation of the inhibition effect of Montelukast Sodium on the copper corrosion in 0.5 mol/L H_2SO_4. *J. Mol. Liq.* **2017**, *248*, 902–910. [CrossRef]
9. Habeeb, H.J.; Luaibi, H.M.; Abdullah, T.A.; Dakhil, R.M.; Kadhum, A.A.H.; Al-Amiery, A. Case study on thermal impact of novel corrosion inhibitor on mild steel. *Case Stud. Therm. Eng.* **2018**, *12*, 64–68. [CrossRef]
10. Al-Baghdadi, S.B.; Hashim, F.G.; Salam, A.Q.; Abed, T.K.; Gaaz, T.S.; Al-Amiery, A. Synthesis and corrosion inhibition application of NATN on mild steel surface in acidic media complemented with DFT studies. *Results Phys.* **2018**, *8*, 1178–1184. [CrossRef]
11. Kadhum, A.; Mohamad, A.; Hammed, L.; Al-Amiery, A.; San, N.; Musa, A. Inhibition of mild steel corrosion in hydrochloric acid solution by new coumarin. *Materials* **2014**, *7*, 4335–4348. [CrossRef]
12. Mohamad, A.B.; Kadhum, A.A.H.; Al-Amiery, A.A.; Ying, L.C.; Musa, A.Y. Synergistic of a coumarin derivative with potassium iodide on the corrosion inhibition of aluminum alloy in 1.0 NH_2SO_4. *Met. Mater. Int.* **2014**, *20*, 459–467. [CrossRef]
13. Al-Amiery, A.; Kadhum, A.; Alobaidy, A.H.; Mohamad, A.; Hoon, P. Novel corrosion inhibitor for mild steel in HCl. *Materials* **2014**, *7*, 662–672. [CrossRef] [PubMed]
14. Al-Amiery, A.; Kadhum, A.; Mohamad, A.; Musa, A.; Li, C. Electrochemical study on newly synthesized chlorocurcumin as an inhibitor for mild steel corrosion in hydrochloric acid. *Materials* **2013**, *6*, 5466–5477. [CrossRef] [PubMed]
15. Kadhum, A.; Al-Amiery, A.; Shikara, M.; Mohamad, A. Synthesis, structure elucidation and DFT studies of new thiadiazoles. *Int. J. Physi. Sci.* **2011**, *6*, 6692–6697.
16. Kelland, M.A. Production chemicals for the oil and gas industry. *Chromatographia* **2010**, *72*, 199.

17. Eddy, N.O.; Ebenso, E.E.; Ibok, U.J. Adsorption, synergistic inhibitive effect and quantum chemical studies of ampicillin (AMP) and halides for the corrosion of mild steel in H_2SO_4. *J. Appl. Electrochem.* **2010**, *40*, 445–456. [CrossRef]
18. Yaro, A.S.; Khadom, A.A.; Wael, R.K. Apricot juice as green corrosion inhibitor of mild steel in phosphoric acid. *Alex. Eng. J.* **2013**, *52*, 129–135. [CrossRef]
19. Li, X.; Deng, S.; Fu, H. Triazolyl blue tetrazolium bromide as a novel corrosion inhibitor for steel in HCl and H_2SO_4 solutions. *Corros. Sci.* **2011**, *53*, 302–309. [CrossRef]
20. Jacob, K.S.; Parameswaran, G. Corrosion inhibition of mild steel in hydrochloric acid solution by Schiff base furoin thiosemicarbazone. *Corros. Sci.* **2010**, *52*, 224–228. [CrossRef]
21. Obot, I.B.; Obi-Ebbedi, N.O. Adsorption properties and inhibition of mild steel corrosion in sulfuric acid solution by ketoconazole: Experimental and theoretical investigation. *Corros. Sci.* **2010**, *52*, 198–204. [CrossRef]
22. Kumar, S.L.A.; Gopiraman, M.; Kumar, M.S.; Sreekanth, A. 2-Acetylpyridine-N(4)-Morpholine Thiosemicarbazone (HAcpMTSc) as a Corrosion Inhibitor on Mild Steel in HCl. *Ind. Eng. Chem. Res.* **2011**, *50*, 7824–7832. [CrossRef]
23. Singh, D.D.N.; Singh, M.M.; Chaudhary, R.S.; Agrawal, C.V. Inhibitive effects of isatin, thiosemicarbazide and isatin-3-(3-thiosemicarbazone) on the corrosion of aluminium alloys in nitric acid. *J. Appl. Electrochem.* **1980**, *10*, 587–592. [CrossRef]
24. Aytac, A.; Ozmen, U.; Kabasakaloglu, M. Investigation of some Schiff bases as acidic corrosion of alloy AA3102. *Mater. Chem. Phys.* **2005**, *89*, 176–181. [CrossRef]
25. Li, S.L.; Ma, H.Y.; Lei, S.B.; Yu, R.; Chen, S.H.; Liu, D.X. Inhibition of copper corrosion with Schiff base derived from 3-methoxysalicylaldehyde and O-phenyldiamine in chloride media. *Corrosion* **1998**, *54*, 947. [CrossRef]
26. Li, S.; Chen, S.; Lei, S.; Ma, H.; Yu, R.; Liu, D. Investigation on some Schiff bases as HCl corrosion inhibitors for copper. *Corros. Sci.* **1999**, *41*, 1273–1287. [CrossRef]
27. Fouda, A.S.; Madkour, L.H.; El-Shafei, A.A.; Abd Elmaksoud, S.A. Corrosion inhibitor for Zinc in 2 M HCl solution. *Bull. Korean Chem. Soc.* **1995**, *16*, 454–458.
28. Lashgari, M.; Arshadi, M.R.; Miandari, S. The enhancing power of iodide on corrosion prevention of mild steel in the presence of a synthetic soluble Schiff base: Electrochemical and surface analyses. *Electrochim. Acta* **2010**, *55*, 6058–6063. [CrossRef]
29. Küstü, C.; Emregül, K.C.; Atakol, O. Schiff bases of increasing complexity as mild steel corrosion inhibitors in 2 M HCl. *Corros. Sci.* **2007**, *49*, 2800–2814.
30. Asan, A.; Kabasakaloglu, M.; Isıklan, M.; Kılıc, Z. Corrosion inhibition of brass in presence of terdentate ligands in chloride solution. *Corros. Sci.* **2005**, *47*, 1534–1544. [CrossRef]
31. El Azhar, M.; Mernari, B.; Traisnel, M.; Bentiss, F.; Lagrenée, M. Corrosion inhibition of mild steel by the new class of inhibitors [2,5-bis(n-pyridyl)-1,3,4-thiadiazoles] in acidic media. *Corros. Sci.* **2001**, *43*, 2229–2238. [CrossRef]
32. Alobaidy, A.; Kadhum, A.; Al-Baghdadi, S.; Al-Amiery, A.; Kadhum, A.; Yousif, E. Eco-friendly corrosion inhibitor: Experimental studies on the corrosion inhibition performance of creatinine for mild steel in HCl complemented with quantum chemical calculations. *Int. J. Electrochem. Sci.* **2015**, *10*, 3961–3972.
33. Amin, M.A.; Ibrahim, M.M. Corrosion and corrosion control of mild steel in concentrated H_2SO_4 solutions by a newly synthesized glycine derivative. *Corros Sci.* **2011**, *53*, 873–885. [CrossRef]
34. Salman, T.A.; Zinad, D.S.; Jaber, S.H.; Al-Ghezi, M.; Mahal, A.; Takriff, M.S.; Al-Amiery, A.A. Effect of 1,3,4-Thiadiazole Scaffold on the Corrosion Inhibition of Mild Steel in Acidic Medium: An Experimental and Computational Study. *J. Bio Tribo Corros.* **2019**, *5*, 1–11. [CrossRef]
35. Kadhim, A.; Al-Okbi, A.K.; Jamil, D.M.; Qussay, A.; Al-Amiery, A.A.; Gaaz, T.S. Experimental and theoretical studies of benzoxazines corrosion inhibitors. *Results Phys.* **2017**, *7*, 4013–4019. [CrossRef]
36. Jamil, D.M.; Al-Okbi, A.K.; Al-Baghdadi, S.B.; Al-Amiery, A.A.; Kadhim, A.; Gaaz, T.S. Experimental and theoretical studies of Schiff bases as corrosion inhibitors. *Chem. Cent. J.* **2018**, *12*, 1–7. [CrossRef] [PubMed]
37. ASTM, G. *Standard Practice for Preparing, Cleaning and Evaluating Corrosion Test Specimens*; American Society for Testing and Materials: West Conshohocken, PA, USA, 2003.
38. Herrag, L.; Hammouti, B.; Elkadiri, S.; Aouniti, A.; Jama, C.; Vezin, H. Adsorption properties and inhibition of mild steel corrosion in hydrochloric solution by some newly synthesized diamine derivatives: Experimental and theoretical investigations. *Corros. Sci.* **2010**, *52*, 3042–3051. [CrossRef]

39. Frisch, M.; Trucks, G.; Schlegel, H.B.; Scuseria, G.; Robb, M.; Cheeseman, J. *Gaussian 09, Revision A 02'*; Gaussian, Inc.: Wallingford, CT, USA, 2009; Volume 200, p. 28.
40. Juttner, K. Electrochemical impedance spectroscopy (EIS) of corrosion processes on inhomogeneous surfaces. *Electrochim. Acta* **1990**, *35*, 1501–1508. [CrossRef]
41. Park, J.R.; Macdonald, D.D. Impedance studies of the growth of porous magnetite films on carbon steel in high temperature aqueous systems. *Corros. Sci.* **1983**, *23*, 295–315. [CrossRef]
42. Walter, G.W. A comparison of single frequency and wide frequency range impedance tests for painted metals. *Corros. Sci.* **1990**, *30*, 617–629. [CrossRef]
43. Walter, G.W. The application of impedance methods to study the effects of water uptake and chloride ion concentration on the degradation of paint films—I. Attached films. *Corros. Sci.* **1991**, *32*, 1059–1084. [CrossRef]
44. Mansfeld, F. Electrochemical impedance spectroscopy (EIS) as a new tool for investigating methods of corrosion protection. *Electrochim. Acta* **1990**, *35*, 1533–1544. [CrossRef]
45. Mendonça, G.L.; Costa, S.N.; Freire, V.N.; Casciano, P.N.; Correia, A.N.; de Lima-Neto, P. Understanding the corrosion inhibition of carbon steel and copper in sulphuric acid medium by amino acids using electrochemical techniques allied to molecular modelling methods. *Corros. Sci.* **2017**, *115*, 41–55. [CrossRef]
46. Ebenso, E. Effect of halide ions on the corrosion inhibition of mild steel in H_2SO_4 using methyl red: Part 1. *Bull. Electrochem.* **2003**, *19*, 209–216.
47. Khamis, A.; Saleh, M.; Awad, M. The counter ion influence of cationic surfactant and role of chloride ion synergism on corrosion inhibition of mild steel in acidic media. *Int. J. Electrochem. Sci.* **2012**, *7*, 10487–10500.
48. Obot, I.; Obi-Egbedi, N.; Umoren, S. Antifungal drugs as corrosion inhibitors for aluminium in 0.1 M HCl. *Corros. Sci.* **2009**, *51*, 1868–1875. [CrossRef]
49. Ju, H.; Kai, Z.-P.; Li, Y. Aminic nitrogen-bearing polydentate Schiff base compounds as corrosion inhibitors for iron in acidic media: A quantum chemical calculation. *Corros. Sci.* **2008**, *50*, 865–871. [CrossRef]
50. Obayes, H.R.; Al-Amiery, A.A.; Alwan, G.H.; Abdullah, T.A.; Kadhum, A.A.H.; Mohamad, A.B. Sulphonamides as corrosion inhibitor: Experimental and DFT studies. *J. Mol. Struct.* **2017**, *1138*, 27–34. [CrossRef]
51. Al-Azawi, K.F.; Al-Baghdadi, S.B.; Mohamed, A.Z.; Al-Amiery, A.A.; Abed, T.K.; Mohammed, S.A. Synthesis, inhibition effects and quantum chemical studies of a novel coumarin derivative on the corrosion of mild steel in a hydrochloric acid solution. *Chem. Cent. J.* **2016**, *10*, 1–11. [CrossRef]
52. Sanap, S.; Patil, R.; Dubey, R. Corrosion Inhibition of Mild Steel by Using Mixed Ligand Metal Complexes. *Int. J. Chem. Sci.* **2013**, *11*, 503–517.
53. Al-Amiery, A.; Kadhum, A.; Kadihum, A.; Mohamad, A.; How, C.; Junaedi, S. Inhibition of mild steel corrosion in sulfuric acid solution by new Schiff base. *Materials* **2014**, *7*, 787–804. [CrossRef]
54. Junaedi, S.; Kadhum, A.; Al-Amiery, A.; Mohamad, A.; Takriff, M. Synthesis and characterization of novel corrosion inhibitor derived from oleic acid: 2-Amino 5-Oleyl-1, 3, 4-Thiadiazol (AOT). *Int. J. Electrochem. Sci.* **2012**, *7*, 3543–3554.
55. Al-Amiery, A.; Al-Majedy, Y.; Kadhum, A.; Mohamad, A. New coumarin derivative as an eco-friendly inhibitor of corrosion of mild steel in acid medium. *Molecules* **2015**, *20*, 366–383. [CrossRef] [PubMed]